Original paper

Image quality and dose evaluation of MVCT TomoTherapy acquisitions: A phantom study

P. De Marco[a,*], I. Abdi Osman[b], F. Castellini[c], R. Ricotti[c,1], M.C. Leonardi[c], E. Miglietta[c],
R. Cambria[a], D. Origgi[a], B.A. Jereczek-Fossa[c,d], C. Garibaldi[e,2], F. Cattani[a,2]

[a] IEO, European Institute of Oncology IRCCS, Unit of Medical Physics, Milan, Italy
[b] University of Milan, Milan, Italy
[c] IEO, European Institute of Oncology IRCCS, Department of Radiation Oncology, Milan, Italy
[d] University of Milan, Department of Oncology and Hemato-Oncology, Milan, Italy
[e] IEO, European Institute of Oncology IRCCS, Radiation Research Unit, Milan, Italy

ABSTRACT

Background: The aim of this study is to evaluate the dose delivered and the image quality of pre-treatment MVCT images with Hi-Art TomoTherapy system, varying acquisition and reconstruction parameters.

Materials and methods: Catphan 500 MVCT images were acquired with all acquisition pitch and reconstruction intervals; image quality was evaluated in terms of noise, uniformity, contrast linearity, contrast-to-noise ratio (CNR) and spatial resolution with the Modulation Transfer Function (MTF).

Dose was evaluated as Multi Slice Average Dose (MSAD$_w$) and measurements were performed with the Standard TomoTherapy® Quality Assurance Kit composed by the TomoTherapy Phantom, the Exradin A1SL ion chamber and TomoElectrometer. For each pitch-reconstruction interval, acquisitions were repeated 5 times.

Results: Differences in noise and uniformity, though statistically significant in some cases, were very small: noise ranged from 2.3% for Coarse – 3 mm to 2.4% for Coarse – 6 mm, while uniformity passed from 99.5% for Coarse – 6 mm to 99.8% for Normal – 4 mm.

No differences at all were found for CNR for high and low density inserts, while MTF was higher for pitch Coarse, even if no differences in spatial resolution were observed visually (spatial resolution was up to 4 lp/cm for all combinations of pitch and reconstruction interval).

Dose was dependent on pitch, being 1.0 cGy for Coarse, 1.5 cGy for Normal and 2.85 cGy for Fine.

Conclusions: We observed negligible differences in image quality among different pitch and reconstruction interval, thus, considerations regarding pre-treatment imaging modalities should be based only on dose delivered and on the desired resolution along the cranio-caudal axis for image-guided radiotherapy and adaptive radiotherapy purposes.

1. Introduction

Image guided radiotherapy (IGRT) has become routine in radiotherapy centers, since imaging the patient before the treatment offers benefits in monitoring positioning accuracy, set-up uncertainties and inter-fraction anatomy changes [1].

Moreover, pre-treatment images can be used for adaptive radiotherapy (ART) allowing physicians to modify the treatment plan during the course of radiotherapy in order to account for anatomical and biological changes, if a reliable calibration curve between pixel values (PV) and electron density is applied [2–5].

Imaging systems differ in the X-ray energy used (kilo-voltage, kV or mega-voltage, MV), geometry of the beam (cone beam CB, or fan beam FB), acquisition, and reconstruction algorithm [6].

The TomoTherapy Hi-Art® (Accuray Inc., US) uses MV computed tomography (MVCT), with a fan-beam and a scan mode that allows the user to choose among 3 different pitch ratios that represent Fine, Normal and Coarse mode. The imaging configuration is called "J01", in which the jaws are set on a position of ± 0.5 mm. In this configuration, the reported beam width at the isocenter is of 4.2 mm [7–10].

Pitch affects dose to the patient, scan time, reconstruction interval (RI) and images resolution.

For each pitch, images can be reconstructed with two different RI resulting in 6 different pitch-RI combinations.

Despite the fact that TomoTherapy MVCT is not a novel imaging device, to our knowledge there are no studies assessing a comprehensive evaluation of the image quality obtained with different pitch and reconstruction intervals.

Thus, the aim of this work is to investigate the impact of pitch and reconstruction interval on image quality, evaluated by conventional metrics of image noise, image uniformity, contrast linearity, contrast to noise ratio and spatial resolution.

In addition, dose measurements have been performed with the same scanning and reconstruction parameters to assess differences and reproducibility in dose delivered during imaging.

2. Materials and methods

2.1. Imaging system

The nominal energy of the electron beam used in the imaging modality of TomoTherapy is 3.5 MeV. The image receptor is an arc-shaped xenon detector. A filtered back-projection is used for image reconstruction, the reconstruction pixel matrix is 512x512 and the display field of view (DFOV) is 400 mm (pixel dimension equal to 0.78 mm).

Before scanning, user can choose among 3 pitches, corresponding to a couch speed of 4, 8 and 12 mm/gantry rotation for pitch *Fine, Normal and Coarse*, respectively. For each pitch, images can be reconstructed with two different RI: with *Coarse* images can be reconstruct with a RI of 6 and 3 mm, with *Normal* RI of 4 and 2 mm can be obtained, while with *Fine* the available RI are 2 and 1 mm.

2.2. Image quality

MVCT image quality was assessed in terms of noise, uniformity, contrast linearity, contrast-to-noise ratio and spatial resolution, expressed using the modulation transfer function (MTF).

A phantom (Catphan 500, Phantom Laboratory, Salem, NY, US) was acquired and images were reconstructed with the 6 different pitch-RI combinations available. Note that the reconstruction thickness must be set prior the acquisition, since it is not possible to perform a *retro*-reconstruction with the same acquired data set.

For each pitch-slice thickness combination, the phantom was scanned 5 times, for a total of 30 acquisitions.

Images were analyzed using ImageJ software (National Institutes of Health, NIH, US) [11]. For each acquisitions a proper number of slices was considered for the analysis of noise, signal uniformity, contrast linearity and contrast-to-noise ratio, in order to take into account a similar scan extension of the phantom, varying from 18 to 20 mm: for 6, 3, 2, 1 mm RI, an extension of 18 mm was considered, so 3, 6, 9 and 18 slices were analyzed, respectively, while for 4 mm RI, 5 slices were analyzed for an extension of 20 mm.

For the assessment of spatial resolution, only the slice with the maximum intensity of the inserts was evaluated.

Image noise and signal uniformity were investigated using the uniformity insert of the Catphan (CTP 486).

Image noise was assessed in a region of interest (ROI) of 120x120 pixels, mean (μ) and standard deviation (σ) of the PV were calculated and noise N was expressed as the ratio σ/μ. For each pitch-RI combination, noise was averaged over all slices and acquisitions and the result expressed as $\bar{N} \pm s_{\bar{N}}$.

Signal uniformity was evaluated placing 5 ROIs 30x30 pixels, 1 at the center and 4 at the periphery, as shown in Fig. 1c. For each slice a uniformity index (UI) was calculated [7,9]

$$UI (\%) = [1 - (Max - Min)/(Max + Min)] \times 100$$

and averaged over all slices and acquisitions. The result was expressed as $\bar{UI} \pm s_{\bar{UI}}$ where $\bar{UI}$ and $s_{\bar{UI}}$ represent the mean and the standard deviation, respectively.

Contrast linearity and contrast-to-noise ratio were investigated using the densitometry insert of the Catphan (CTP 404). The insert contains 6 different materials (PMP, LDPE, Polystyrene, Acrylic, Delrin and Teflon) with relative electron densities ranging from 0.853 to 1.868. An additional insert contains air (relative electron density 0.001). Circular ROIs were placed at each insert (see Fig. 1a) and mean PV was considered to build the curves PV-relative electron density for each acquisition and reconstruction.

In addition, 2 ROIs were placed on the background near the Delrin and the Polystyrene inserts (see Fig. 1b), to calculate the contrast-to-noise ratio as follow:

$$CNR = \frac{\mu_{ins} - \mu_{BG}}{\sigma_{BG}}$$

CNR was calculated for each slice and averaged over all slices and all acquisitions.

Spatial resolution was evaluated in terms of Modulation Transfer Function using the method proposed by Droege [12]. For each set of images, only the slice in which the inserts were most visible was analyzed.

MTF values corresponding to each spatial frequency were averaged over the 5 acquisitions for each pitch-RI combinations.

2.3. Dose assessment

Evaluation of the Multi Slice Average Dose (MSAD$_w$) was performed with the Standard TomoTherapy® Quality Assurance Kit composed by the Tomotherapy Phantom, the Exradin A1SL ion chamber (Standard Imaging, Middleton, WI) and a TomoElectrometer [13].

Measurements were performed according to the Report of AAPM Task Group 148 [8], thus with no correction due to spectral changes between imaging and treatment beam.

For each position of the ion chamber inside the phantom, measurements were repeated 5 times for each of the 6 pitch-RI combinations. Measurements were performed with 2 different scan lengths (5 and 10 cm) and MSAD$_w$ was calculated according to the formula [7,10]

$$MSAD_w = \frac{1}{3} \times D_{center} + \frac{2}{3} \times D_{periphery}$$

where D$_{center}$ is the absorbed dose measured at the center of the phantom, while D$_{periphery}$ is the average of the doses measured in the 4 points at the periphery of the phantom.

For each position, coefficient of variation (COV) of the 5 consecutive measurements was calculated as ratio between standard deviation and mean.

In addition, ratio MSAD$_w^{5cm}$/MSAD$_w^{10cm}$ was calculated for each pitch-RI combination.

2.4. Statistical analysis

Normality of data was assessed using Shapiro-Wilk test and for each investigated parameter (image noise, uniformity and contrast-to-noise ratio) an unpaired *t*-test with Bonferroni correction for multiple comparison was performed to evaluate whether differences among pitch-RI combinations have statistical significance [14]. A p-value of 0.05 was chosen as threshold.

For contrast linearity, data were fitted using a linear model and 95% confidence intervals were considered for slopes and intercepts for all pitch-RI combinations.

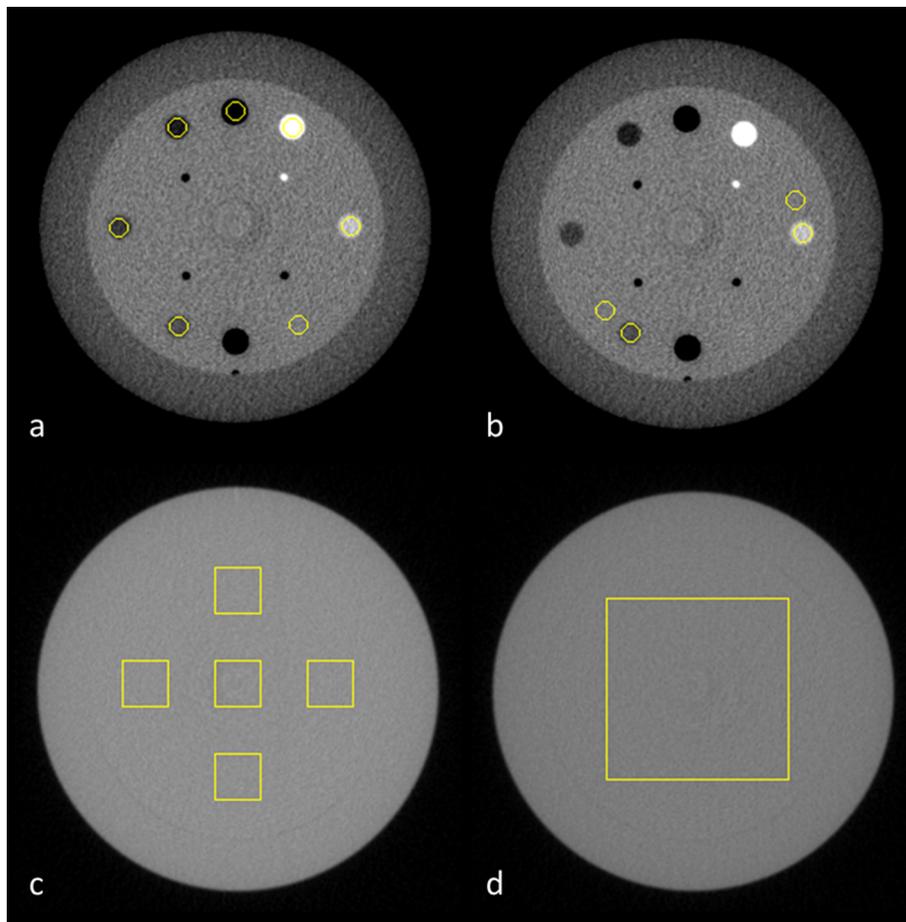Analysis was performed using R-software, version 3.5.1 [15].

Fig. 1. MVCT images of the Catphan: ROIs for contrast linearity (a), contrast-to-noise ratio (b), image uniformity (c) and image noise (d) are shown in yellow.

3. Results

3.1. Image quality

Image noise changed slightly from 2.42% for C-6 (*Coarse* – 6 mm), to 2.32% for C-3 (*Coarse* – 3 mm), but this difference was statistically significant (p < 0.05). For pitch *Normal* and *Fine* the differences between the 2 reconstruction thickness were lower, as shown in Table 1. P-values for all pitch-RI combinations are shown in Table 2.

Signal uniformity varied from 99.5% to 99.8% passing from C-6 to C-3 and N-4 (see Table 1) and this difference was statistically significant.

Contrast-to-noise ratios for Delrin (mimicking bone) and Polystirene (mimicking soft tissue) varied from 7.2 and 7.5 and from 4.3 and 4.1, respectively (see boxplots in Fig. 2, in which n refers to the number of slices analyzed). In both cases, differences among pitch-RI combinations were not statistically significant (p > 0.05).

Linearity between pixel values evaluated on the images and the relative electron density of the various inserts was strongly assessed ($R^2 > 0.99$), for every pitch-RI combination.

Curve obtained with pitch *Coarse* and RI of 6 mm was different from those obtained on average with other pitch-RI combinations: 95% confidence interval for the slopes of *Coarse* – 6 mm was 867.7–874.4 PV, while for the other pitch-RI combinations the inferior limit of the confidence interval ranged from 870.5 to 875.7 PV and the superior limit ranged from 880.9 to 885.5 PV (the average 95% confidence interval was 873.3–883.6 PV).

Greatest differences among curves were observed for *Coarse* – 6 mm and *Normal* – 4 mm, as shown in Fig. 3.

Quantitative evaluation of spatial resolution, in terms of $MTF_{50\%}$, is shown in table 3. A trend related to the acquisition pitch can be observed: spatial resolution seems to be higher for pitch *Coarse* and decreases for lower pitch.

Qualitative evaluation, however, provided no differences among pitch-RI combinations, as the inserts were clearly visible up to 4 lp/cm, as shown in Fig. 4.

3.2. Dose assessment

Dose values for different pitch-RI-scan lengths combinations are shown in Table 4. Measured dose depended on scanning pitch: from *Coarse* to *Normal*, dose increased of about 50%, while from *Coarse* to *Fine* dose was about 3-times higher.

Due to the higher amount of scattered radiation, MSAD for the 10 cm scan length was higher and the ratio $MSAD_w^{5cm}/MSAD_w^{10cm}$ was in the range 0.91–0.94, depending on scanning pitch.

High reproducibility of dose measurements across pitch, scan

Table 1

Image noise and image uniformity for different pitch-reconstruction interval combinations.

Pitch – reconstruction interval	Image Noise (mean ± SD)	Image Uniformity (mean ± SD)
Coarse – 6 mm	2.42% ± 0.02%	99.54% ± 0.07%
Coarse – 3 mm	2.32% ± 0.03%	99.83% ± 0.05%
Normal – 4 mm	2.33% ± 0.03%	99.83% ± 0.04%
Normal – 2 mm	2.37% ± 0.05%	99.64% ± 0.07%
Fine – 2 mm	2.39% ± 0.02%	99.63% ± 0.09%
Fine – 1 mm	2.38% ± 0.02%	99.65% ± 0.10%

Table 2
p-value matrix for image noise analysis (upper part, underlined) and uniformity analysis (lower part, italic).

	Coarse – 6 mm	Coarse – 3 mm	Normal – 4 mm	Normal – 2 mm	Fine – 2 mm	Fine – 1 mm
Coarse – 6 mm	\	< 0.05	< 0.05	< 0.05	< 0.05	< 0.05
Coarse – 3 mm	< 0.05	\	0.23	< 0.05	< 0.05	< 0.05
Normal – 4 mm	< 0.05	0.97	\	< 0.05	< 0.05	< 0.05
Normal – 2 mm	< 0.05	< 0.05	< 0.05	\	< 0.05	< 0.05
Fine – 2 mm	< 0.05	< 0.05	< 0.05	0.45	\	< 0.05
Fine – 1 mm	< 0.05	< 0.05	< 0.05	0.71	0.27	\

length, slice thickness and position was observed: COV was below 1% in 52 repeated measurements out of 60 and the highest was of 1.8%.

Dose in central position was of 0.96 cGy for pitch *Coarse*, 1.43 cGy for pitch *Normal* and 2.82 cGy for pitch *Fine* with 10 cm scan length.

For 5 cm scan length, instead, central dose was of 0.87 cGy, 1.27 cGy and 2.46 cGy for pitch *Coarse*, *Normal* and *Fine*, respectively.

4. Discussion

In this work we have investigated the impact of pitch and reconstruction interval on phantom image quality, evaluating conventional metrics of image noise, image uniformity, contrast linearity, contrast to noise ratio and spatial resolution. Moreover, differences and reproducibility in delivered imaging dose was assessed as a function of scanning and reconstruction parameters.

4.1. Image quality

According to our results, images were less noisy and presented more uniformity using *Coarse* – 3 mm and *Normal* – 4 mm. Despite the statistical significance (see Tables 3), noise range was very narrow (2.32% − 2.42%), as uniformity range (99.54% − 99.83%) with no clear trend among acquisition pitch or reconstruction interval.

Acquisition pitch and reconstruction interval had no impact on contrast-to-noise ratio for the considered materials.

Linearity between mean PV and relative electron density was achieved among all acquisition pitch-RI combinations and the observed differences between modalities of acquisition/reconstruction, although

statistically significant, were very small in terms of calculated electron density and negligible in terms of dose calculations. In fact, for a given PV, the difference in the relative electron density was always below 2%: this small difference brings a negligible variation in dose calculation if the imaging parameters are different from those used for the calculation of the calibration curve [2,16,17].

Qualitative evaluation of spatial resolution provided values of 4 lp/cm for all pitch-RI combinations, different values of the $MTF_{50\%}$ did not reflect the fact that resolution was degraded very fast for bar patterns above 5 lp/cm, thus image quality did not vary according to the calculated MTF values.

Chan et al. [19] compared different image guidance system with a Catphan 500 and found noise of 2.8%, spatial resolution in the range 3–5 lp/cm and image uniformity of 99.7% with the MVCT acquisition with pitch *Normal* and 4 mm slice thickness, in close agreement with values we found.

Jung et al. [9] acquired an AAPM CT phantom with different parameters and found a noise of 2.8% and a uniformity above 99.8% for the 3 pitch involved, whose results are comparable to those we presented.

Fast et al. [20] reported a $MTF_{50\%}$ of 2.1 lp/cm measured with a ConeBeam phantom, while Held et al. [21] found a $MTF_{50\%}$ of 2.1 lp/cm with a Catphan 500 and image noise of 3.14% with pitch *Normal* and 2 mm reconstruction thickness, compared to our 2.7 lp/cm and 2.37%, respectively.

These differences in spatial resolution might be related to the methods used for the calculation of the MTF.
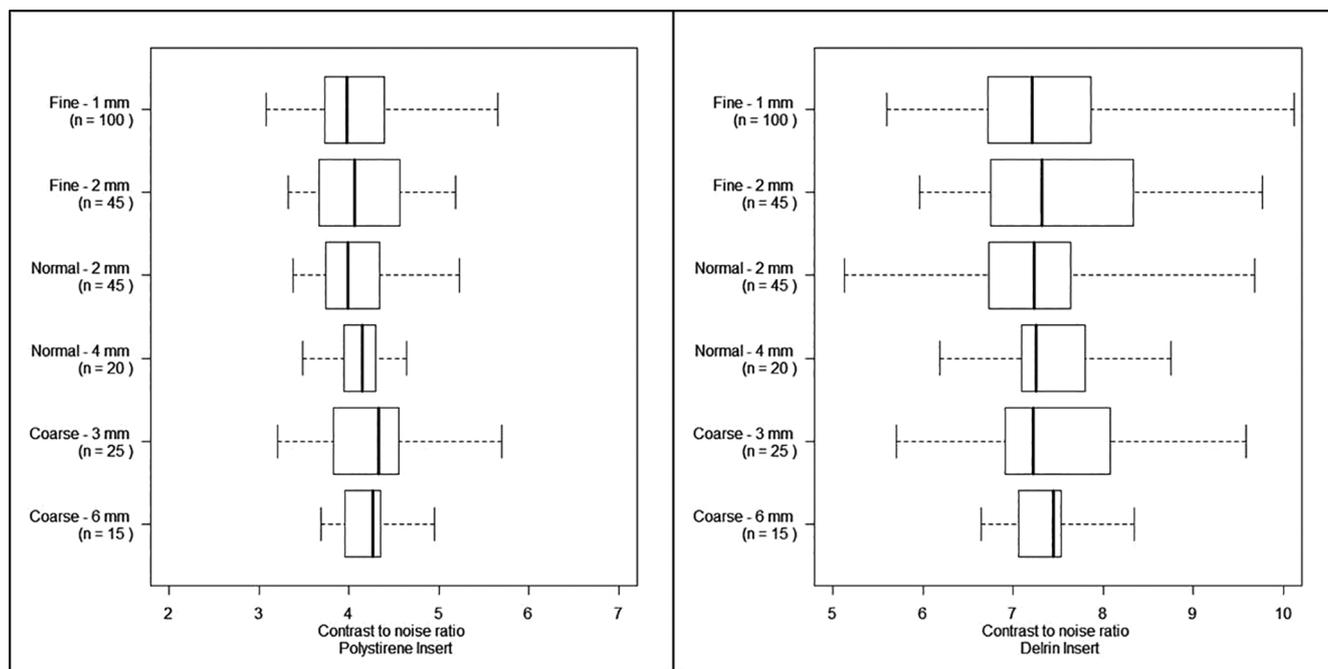

Fig. 2. Results for Contrast-to-noise ratio for Delrin and Polystirene.
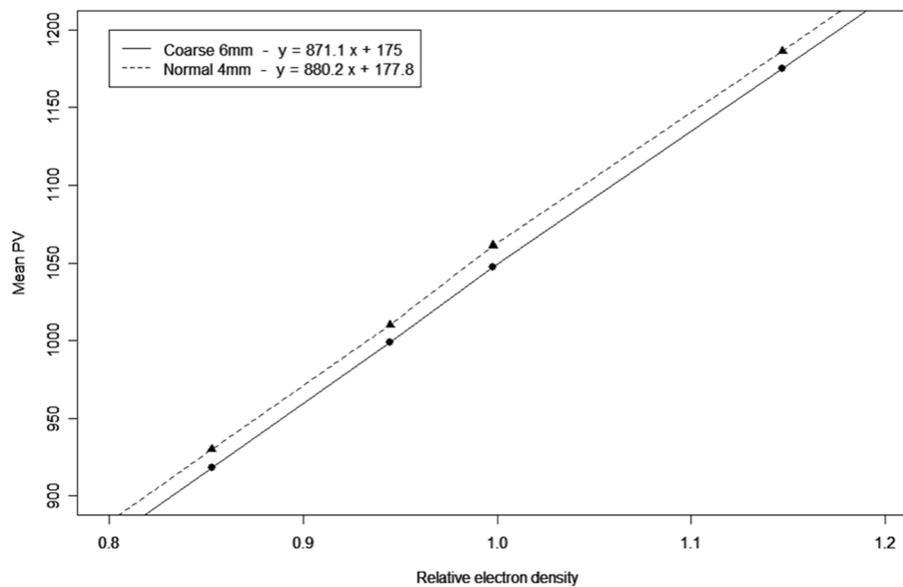
Fig. 3. Mean PV for PMP, LDPE, Polystirene and Acrylic as a function of their relative electron density for *Coarse* 6 mm and *Normal* 4 mm.

Table 3
MTF 50% for different pitch-reconstruction interval combinations.

Pitch – Reconstruction Interval combination	MTF$_{50\%}$ (lp/cm)
Coarse – 6 mm	3.34 ± 0.32
Coarse – 3 mm	3.35 ± 0.33
Normal – 4 mm	2.66 ± 0.16
Normal – 2 mm	2.66 ± 0.29
Fine – 2 mm	2.49 ± 0.16
Fine – 1 mm	2.46 ± 0.14

4.2. Dose assessment

Measured MSAD$_w$ varied greatly with acquisition pitch: passing from *Coarse* to *Normal*, the increase was about 45%, while the measured dose with pitch *Fine* was two-fold higher than with pitch *Normal* and three-fold higher than with pitch *Coarse*. MSAD$_w$ were dependent of acquisition pitch only, as expected.

Our results are in agreement with values published by Mege et al. [13] who reported a MSAD$_w$ of 3 cGy, 1.5 cGy and 1.1 cGy for pitch *Fine*, *Normal* and *Coarse*, respectively.

As shown in Table 5, with the same detector, phantom and scan length, results by Mege et al. [10] are close to our values (within ± 4%).

Considering the results of Jung et al. [9], differences were in the range 5%-13%, depending on acquisition pitch, while the calculations of Chen et al. [18] provided lower values for pitch *Fine* and *Normal* (differences of 11–13%).

We found a relative dose variation with the scan length in agreement with that obtained by Mege et al. [10], who reported a ratio of about 0.9 between central dose with 5 and 10 cm scan length. Our ratios were of 0.91, 0.89 and 0.87 for pitch *Coarse*, *Normal* and *Fine*, respectively.

4.3. Clinical impact

We demonstrated that acquisition pitch and reconstruction interval did not affect transverse image quality in terms of noise, uniformity and contrast-to-noise ratio, while the observed differences in the MTF among pitches did not find correspondence on the images, in which the 4 lp/cm insert was always detectable.

In addition, the statistical significant difference of the curve PV-

electron density leads to negligible variation in dose calculation.

As shown previously, dose due to the pre-treatment imaging depended only on acquisition pitch, with typical values of 1 cGy, 1.5 cGy and 3 cGy for pitch *Coarse*, *Normal*, and *Fine*, respectively.

Pre-treatment imaging may lead to non-negligible dose to patients, as shown extensively by Alaei et al.[22], thus acquisition modality should be tailored according to a good balance between exposure and clinical impact on the treatment.

The choice of acquisition pitch and reconstruction interval is crucial for the accuracy of patient positioning in IGRT, and even more important for ART, Indeed, they may affect image registration for IGRT and dose calculation for ART [23].

According to Zhu et al. [3], when there is no impact on IGRT image quality and ART accuracy, largest pitch should be used to maintain the additional dose to the patient as low as possible.

Langen et al. [2,24] demonstrated that, even when the variation of HU was not negligible, the dose calculation was not affected significantly.

However, if we consider the accuracy of registration, larger pitch and larger reconstruction interval would lead to larger error, especially in cranio-caudal direction, and these errors are greater for chest than for pelvis, as shown in previous reports [3,25]. The trade-off between accuracy for IGRT/ART and imaging dose depends on the fractionation scheme used.

Zhu et al. [3] recommend *Normal* pitch and RI of 2 mm as trade-off between IGRT and ART, while for stereotactic radiotherapy of lung tumors, pitch *Fine* and RI 1 mm was recommended, in order to avoid loss of critical target anatomy information and tumor density [3,26,27].

Relying on the results of Zhu et al. [3], the errors induced by acquisition with a large pitch, might be reduced to a submillimeter value using the "Full image" registration technique.

According to this, we recommend a *Coarse* pitch with a reconstruction interval of 3 mm as a trade-off among accuracy for IGRT and ART and additional dose delivered to patient.

Since our work has been conducted on a cylindrical phantom, further studies on anthropomorphic-shaped phantom should be performed to confirm these results.

In addition, further studies regarding 2D dose distribution with Gafchromic films [10,28] or TLD [10] could be helpful in the complete characterization of the MVCT imaging technique, since current literature presents few works with different results [10,29].
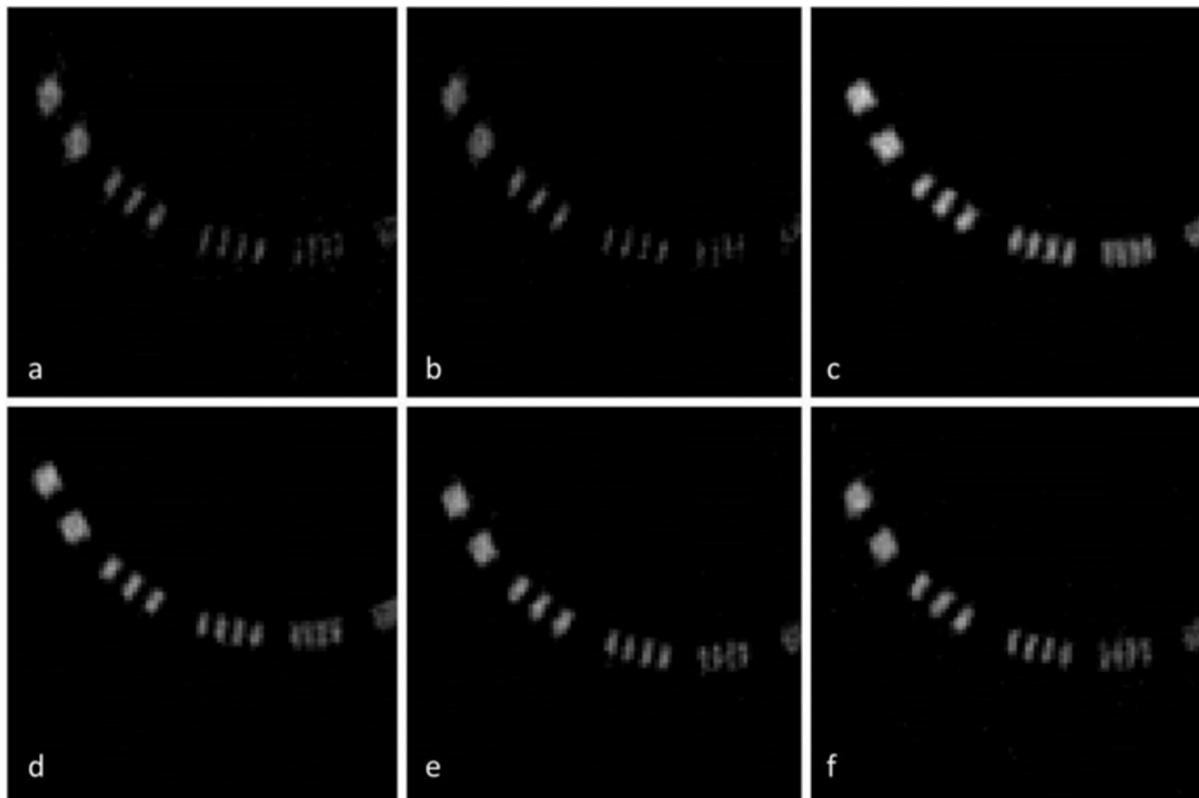
Fig. 4. Visual representation with the same window and level of the spatial resolution insert of Catphan for *Coarse* – 3 mm (a), *Coarse* – 6 mm (b), *Fine* – 1 mm (c), *Fine* – 2 mm (d), *Normal* – 2 mm (e) and *Normal* – 4 mm (f).

Table 4
MSAD$_w$ for different pitch-RI-scan lengths combinations.

Pitch/RI	MSAD$_w$ 10 cm (cGy) (mean $\pm$ 2 SD)	MSAD$_w$ 5 cm (cGy) (mean $\pm$ 2 SD)
FINE – 2 mm	2.83 $\pm$ 0.01	2.67 $\pm$ 0.01
FINE – 1 mm	2.84 $\pm$ 0.02	2.67 $\pm$ 0.01
NORMAL – 4 mm	1.48 $\pm$ 0.01	1.38 $\pm$ 0.01
NORMAL – 2 mm	1.48 $\pm$ 0.01	1.36 $\pm$ 0.01
COARSE – 6 mm	1.02 $\pm$ 0.01	0.92 $\pm$ 0.01
COARSE – 3 mm	1.03 $\pm$ 0.01	0.94 $\pm$ 0.01

Table 5
Comparison of different published measured and calculated values for central dose.

	Jung [9]	Chen [18]	Mege [10]	Our results
Detector	A1SL 0.053 cm^3 Standard Imaging	Calculations	A1SL 0.053 cm^3 Standard Imaging	A1SL 0.053 cm^3 Standard Imaging
Phantom	Virtual water	Virtual water	Virtual water	Virtual water
Diameter (cm)	30	30	30	30
Scan length (cm)	10.8	9.6	10.0	10.0
Fine (cGy)	2.69	2.54	2.70	2.82
Normal (cGy)	1.30	1.27	1.40	1.43
Coarse (cGy)	0.85	0.85	1.00	0.96

5. Conclusion

Dose measurements have confirmed the results already published in the literature of ratios 1:1.5:3 passing from pitch *Coarse*, to *Normal* and to *Fine*.

We showed that the change of pitch and/or reconstruction interval has small or no impact at all on image quality and, thus, considerations regarding pre-treatment imaging modalities should be based only on dose delivered and on the desired resolution along the cranio-caudal axis of patients for IGRT and ART purposes.

Conflict of interest

Miglietta E and Ricotti R have received a research grant from Accuray Inc. The sponsor did not play any role in the study design, collection, analysis, and interpretation of data, nor in the writing of the manuscript, nor in the decision to submit the manuscript for publication. All other authors declare that they have no conflict of interest.

References

[1] De Los SJ, et al. Image guided radiation therapy (IGRT) technologies for radiation therapy localization and delivery. Int J Radiat Oncol Biol Phys 2013;87:33–45.
[2] Langen K, et al. The use of megavoltage CT (MVCT) images for dose recomputations. Phys Med Biol 2005;50:4259.
[3] Zhu J, et al. Effects of megavoltage computed tomographic scan methodology on setup verification and adaptive dose calculation in helical TomoTherapy. Radiation Oncology 2018;13:80.
[4] Morin O, et al. Dose calculation using megavoltage cone-beam CT. Int J Radiat Oncol Biol Phys 2007;67(4):1201–10.
[5] Petit SF, et al. Calibration of megavoltage cone-beam CT for radiotherapy dose calculations: correction of cupping artifacts and conversion of CT numbers to electron density. Med Phys 2008;35(3):849–65.
[6] Mackie TR, et al. Megavoltage imaging systems. In: Mundt AJ, Roeske JC, editors.

Image-guided radiation therapy. Shelton, CT: People's Medical Publishing House-USA; 2011. p. 123–9.

[7] Meeks SL, et al. Performance characterization of megavoltage computed tomography imaging on a helical tomotherapy unit. Med Phys 2005;32(8):2673–81.

[8] Langen KM, et al. QA for helical tomotherapy: report of the AAPM Task Group 148. Med Phys 2010;37(9):4817–53.

[9] Jung JH, et al. Effect of jaw size in megavoltage CT on image quality and dose. Med Phys 2012;39(8):4976–83.

[10] Mege JP, et al. Evaluation of MVCT imaging dose levels during helical IGRT: comparison between ion chamber, TLD, and EBT3 films. J Appl Clin Med Phys 2016;17(1):143–57.

[11] Rasband WS, ImageJ, U.S. National Institutes of Health, Bethesda, Maryland, USA, http://imagej.nih.gov/ij/, 1997-2016.

[12] Droege RT, Morin RL. A practical method to measure the MTF of CT scanners. Med Phys 1982;9(5):758–60.

[13] https://www.accuray.com/wp-content/uploads/tt-all-qa-kit-en-mkt-tt-0515-0113.pdf.

[14] Taylor JR. An introduction to error analysis: the study of uncertainties in physical measurements. Cambridge (UK): Cambridge University Press; 1997.

[15] R Development Core Team (2008). R: A language and environment for statistical computing. R Foundation for Statistical Computing, Vienna, Austria. ISBN 3-900051-07-0, URL http://www.R-project.org.

[16] Ruchala KJ, et al. Calibration of a tomotherapeutic MVCT system. Phys Med Biol 2000;45:N27–36.

[17] Hughes J, et al. An investigation into factors affecting electron density calibration for a megavoltage cone-beam CT system. J Appl Clin Med Phys 2012;13(5):93–107.

[18] Chen M, et al. Quantitative characterization of tomotherapy MVCT dosimetry. Med Dosim 2013;38:280–6.

[19] Chan MF, et al. Evaluation of imaging performance of major image guidance systems. Biomed Imaging Interv J 2011;7(2):e11.

[20] Fast MF, et al. Performance characteristics of a novel megavoltage cone-beam-computed tomography device. Phys Med Biol 2012;57:N15–24.

[21] Held M, et al. Assessment of image quality and dose calculation accuracy on kV CBCT, MV CBCT, and MV CT images for urgent palliative radiotherapy treatments. J Appl Clin Med Phys 2016;17(2):279–90.

[22] Alaei P, Spezi E. Imaging dose from cone beam computed tomography in radiation therapy. Phys Med 2015;31(7):647–58.

[23] Branchini M, et al. Validation of a method for "dose of the day" calculation in head-neck tomotherapy by using planning ct-to-MVCT deformable image registration. Phys Med 2017;39:73–9.

[24] Langen KM, et al. Quality assurance of onboard megavoltage computed tomography imaging and target localization systems for on- and off-line image-guided radiotherapy. Int J Radiat Oncol Biol Phys 2008;71:S62–5.

[25] Woodford C, et al. Image registration of a moving target phantom with helical tomotherapy: effect of the CT acquisitions technique and action level proposal. Phys Med Biol 2008;53:5093–106.

[26] Ettinger DS, et al. Non-small cell lung cancer, version 2.2013. J Natl Compr Cancer Netw 2013;11:645–53.

[27] Feng M, et al. Computed tomography number changes observed during computed tomography-guided radiation therapy for head and neck cancer. Int J Radiat Oncol Biol Phys. 2015;91:1041–7.

[28] Cusumano D, et al. Sum signal dosimetry: A new approach for high dose quality assurance with Gafchromic EBT3. J Appl Clin Med Phys 2017;18(2):181–90.

[29] Shah A, et al. Patient dose from megavoltage computed tomography imaging. Int J Radiat Oncol Biol Phys 2008;70(5):1579–87.